



## Catalytic degradation of O-cresol using H<sub>2</sub>O<sub>2</sub> onto Algerian Clay-Na

Hayat Herbache, Amina Ramdani, Zoubida Taleb, Ramiro Ruiz-Rosas, Safia Taleb, Emilia Morallón, Laurence Pirault-Roy, Noredine Ghaffour

### ► To cite this version:

Hayat Herbache, Amina Ramdani, Zoubida Taleb, Ramiro Ruiz-Rosas, Safia Taleb, et al.. Catalytic degradation of O-cresol using H<sub>2</sub>O<sub>2</sub> onto Algerian Clay-Na. Water environment research, 2019, 91 (2), pp.165-174. 10.1002/wer.1022 . hal-02497353

**HAL Id: hal-02497353**

**<https://hal.science/hal-02497353>**

Submitted on 17 Mar 2023

**HAL** is a multi-disciplinary open access archive for the deposit and dissemination of scientific research documents, whether they are published or not. The documents may come from teaching and research institutions in France or abroad, or from public or private research centers.

L'archive ouverte pluridisciplinaire **HAL**, est destinée au dépôt et à la diffusion de documents scientifiques de niveau recherche, publiés ou non, émanant des établissements d'enseignement et de recherche français ou étrangers, des laboratoires publics ou privés.

# Catalytic degradation of O-cresol using H<sub>2</sub>O<sub>2</sub> onto Algerian Clay-Na

Hayat Herbache,<sup>1</sup> Amina Ramdani,<sup>1,2</sup> Zoubida Taleb,<sup>1</sup> Ramiro Ruiz-Rosas,<sup>3</sup> Safia Taleb,<sup>1</sup> Emilia Morallón,<sup>3</sup> Laurence Pirault-Roy,<sup>4</sup> Noredine Ghaffour<sup>5</sup>

<sup>1</sup>Laboratory of Materials & Catalysis, Faculty of Exact Sciences, Djillali Liabès University, Sidi Bel-Abbès, Algeria

<sup>2</sup>Department of Chemistry, Faculty of Sciences, University Dr. Moulay Tahar, Saida, Algeria

<sup>3</sup>Instituto Universitario de Materiales, Universidad de Alicante, Alicante, Spain

<sup>4</sup>Institut de Chimie des Milieux et Matériaux de Poitiers, IC2MP UMR 7285, B27, TSA 51106, Poitiers Cedex, France

<sup>5</sup>Water Desalination & Reuse Centre, King Abdullah University of Science and Technology (KAUST), Division of Biological & Environmental Science & Engineering (BESE), 23955-6900 Thuwal 23955-6900, Saudi Arabia

Correspondence to: Safia Taleb, Laboratory of Materials & Catalysis, Faculty of Exact Sciences, Djillali Liabès University, Sidi Bel-Abbès, Algeria. Email: safiatat@yahoo.fr

the Algerian Directorate General of Scientific Research and Technological Development (DGRSDT); the Ministry for Higher Education and Scientific Research

## • Abstract

Clay material is used as a catalyst to degrade an organic pollutant. This study focused on the O-cresol oxidative degradation in aqueous solution by adding H<sub>2</sub>O<sub>2</sub> and Mont-Na. The catalytic tests showed a high catalytic activity of Mont-Na, which made it possible to achieve more than 84.6% conversion after 90 min of reaction time at 55°C in 23.2 mM H<sub>2</sub>O<sub>2</sub>. The pH value was found to be negatively correlated with the degradation rate of O-cresol. UV-Vis spectrophotometry revealed that the increase of degradation rate at low pH is related to the formation of 2-methylbenzoquinone as intermediate product. In addition, the content of iron in Mont-Na decreased after the catalytic test, bringing further evidence about the O-cresol catalytic oxidation. The mineralization of O-cresol is also confirmed by the different methods of characterization of Mont-Na after the catalytic oxidation test. The effect of the O-cresol oxidation catalyzed by natural clay is significant. © 2018 Water Environment Federation

## • Practitioner points

- Algerian Montmorillonite-Na is used as a catalyst to degrade an organic pollutant: O-cresol.
- It shows a great potential for catalyst properties in the presence of the oxidizing reagent H<sub>2</sub>O<sub>2</sub>.
- It proved to be an effective means for the degradation of O-cresol contained in wastewaters.

- **Key words**

catalytic oxidation; hydrogen peroxide; O-cresol; sodium clay; wastewater

## **Introduction**

Environmental pollution from industrial and agricultural activities results in contaminated waters, posing significant health risks to living species (Gavrilescu, Demnerová, Aamand, Agathos, & Fava, 2015; Hadjar, Hamdi, & Ania, 2011). Therefore, the presence of the chemical pollution and in particular organic compounds, even in small quantities (doses), makes the water unsuitable for human consumption or even toxic (Shivaraman & Pandey, 2000; Tabué Youmbi, Feumba, Njitat, Marsily, & Ekodeck, 2013). Cresols are industrial phenolic products, which can be found as water pollutants. They are colorless solids with a medicinal odor that can be liquid in the case of mixtures (ATSDR, 2008). There are three forms of cresols that differ slightly in their chemical structure: ortho-cresol (O-cresol), meta-cresol (m-cresol), and para-cresol (p-cresol). These forms are presented separately or as a mixture (Vijayakumar, Chikkala, Mandal, & Mayadevi, 2011). They are produced or utilized in oil refineries, pharmaceutical industry, agribusiness, and household disinfectants (William & Roper, 1992; Yi, Zhuang, Wu, Tay, & Tay, 2006). Under the environmental protection laws, several countries have recognized cresols as very toxic phenolic micropollutants by either contact, inhalation, or ingestion, causing serious health and environmental problems (Chena et al., 2016). They appear in several lists of priority hazardous substances, such as those published by the Agency for the Registry of Toxic Substances and Diseases (ATSDR) and the United States Environmental Protection Agency (USEPA) (Lassouane, Amrani, & Aït-Amar, 2013). In addition, the USEPA sets a regulatory framework, which considers cresols as persistent and priority toxic products and show that limit values should not exceed 12 µg/L (Kavitha & Palanivelu, 2005; Shadnia & Wright, 2008). Their allowable mass content in industrial wastewater is not listed in the Algerian regulations. However, that of phenol is published, it must not exceed 1 mg/L in the discharge of water resource recovery facilities and 2 µg/L in treated wastewater used for irrigation purposes (Official Journal of the Algerian Republic No 41, 2012).

Current purification techniques are able to remove most pollutants satisfactorily, but these techniques often have a high cost. Methods for the removal of O-cresol can be classified into two groups: (a) nondestructive methods: coagulation, chemical precipitation, ion exchange, adsorption, ion exchange resins (Huang, 2009; Kennedy, Vijaya, Sekaran, & Kayalvizhi, 2007; Li et al., 2018; Titus, Kalkar, & Gaikar, 2002; Toh, Lim, Seng, & Adnan, 2013; Wang et al., 2015), and membrane processes (Jiang, Zhang, & Yan, 2015; Wernert et al., 2006). (b) Destructive methods: chemical oxidation, electrochemical oxidation, and photocatalytic oxidation (Borji, Nasser, Mahvi, Nabizadeh, & Javadi, 2014; Khunphonoi & Grisdanurak, 2016; Ling et al., 2015; Shahrezaei, Mansouri, Zinatizadeh, & Akhbari, 2012) and biological treatment (Adav, Chen, Lee, & Ren, 2007; Ren, Peng, Zhao, & Wei, 2014). Chemical oxidation presents itself as a technology of choice for the treatment of wastewater, because it is an efficient, simple, and economical process. It can replace biological processes when they are not effective enough (Zaviska, Drogui, Mercier, & Blais, 2009).

Moreover, the adsorption treatment is the technique of choice for the reduction of organic micropollutants.

Several studies have shown that adsorption on clay is easily achievable (Feddal et al., 2014; Hocine, Boufatit, & Khouider, 2004; Kausar et al., 2018; Ramdani, Taleb, Benghalem, Deratani, & Ghaffour, 2015; Sennour, Mimane, Benghalem, & Taleb, 2009), and the combination of both adsorption and chemical oxidation processes has also shown a huge capacity for the abatement of wastewater pollutants, which are not biodegradable, have toxic character and/or present high concentrations (Hernandez-Esparza, Doria-Serrano, Acero Salinas, & Ruiz-Trevino, 2006; Khaki, Shafeeyan, Raman, & Daud, 2017; Salazar-Gil, Díaz-Nava, & Solache-Ríos, 2016). In this sense, the catalytic properties of clay for several reactions with industrial applications (hydrogenation, oxidation, and polymerization) were highlighted several decades ago (Bertella & Pergher, 2015; Saiah, Hachemaoui, & Yahiaoui, 2017). Bridged clays have been studied as a catalyst to remove organic pollutants in the presence of  $H_2O_2$  (Ellias & Sugunan, 2014; Gil, Korili, & Vicente, 2008; Kurian & Sugunan, 2006; Molina, Casas, Zazo, & Rodriguez, 2006). Ammonia, nitrates, dinitrogen, halides, and/or sulfur can be also obtained if nitrogen, sulfur, and/or halogens are found in the formulation of the pollutants (Deng & Englehardt, 2006; Yan, Wu, & Zhang, 2016). The oxidation processes in the liquid phase in the presence of  $H_2O_2$  are known to be highly effective. In the presence of certain metal ions, and more particularly Fe (II), the formation of hydroxyl radicals ( $OH^\bullet$ ) or hydroperoxide ( $HOO^\bullet$ ) takes part leading to the catalytic oxidation of cresol (Adan, Carbajo, Bahamonde, & Martinez-Aias, 2009; Deng & Englehardt, 2006; Yan et al., 2016; Zaviska et al., 2009). It is important to emphasize that the use of this oxidant alone is not effective for most organic products (Lahbabi, Rais, Hajjaji, & Kacim, 2009). Oxidation processes consist in partial or total oxidation to form inorganic by-products, carbon dioxide and water, which are safe and nontoxic to the environment (Navalon, Alvaro, & Garcia, 2010; Zaviska et al., 2009).

Several authors have studied the use of the oxidation processes for the removal of organic pollutants. Thus, Yan et al. (2016) performed a wet catalytic oxidation of phenol using a  $Fe_2O_3$  ( $Fe_2O_3$ /MCM-41) doped zeolite suspension in a fixed bed reactor. The influence of the reaction temperature, the height of the catalyst bed, and the feed rate was optimized. Then, the mechanism of reaction of the wet catalytic oxidation of phenol on  $Fe_2O_3$ /MCM-41 was studied by determining the concentrations of intermediates. The results showed that the conversion rates of phenol,  $H_2O_2$ , and TOC reached 99%, 91%, and 72.5%, respectively, under optimum operating conditions (feed rate of 2.0 ml/min, temperature 80°C, and catalyst bed height of 4 cm). Phenol is converted to benzoquinone, catechol, and hydroquinone.

Kurian and Sugunan (2006) studied the wet peroxide oxidation (WPO) using as catalyst pillared clays with Fe/Al in the presence of  $H_2O_2$ . The results showed a maximum oxidation of phenol of 78%, reached at 15 min and 80°C. In addition, it was demonstrated that there is a synergistic effect between these metals. A mechanism involving the formation of phenoxy radicals on the surface and inside the pores of the catalyst, which then reacts with the peroxide to give OH radical and diphenols as Catechol and hydroquinone. The produced free radical propagates the chain by attacking the phenol molecule, forming diphenols.

In a different work, four types of activated carbon catalysts derived from coconut (SAC), coal tar (PAC), coal (CAC), and oak wood (WAC) were used in the CWPO process for the catalytic oxidation of

m-cresol in wastewater in the presence of H<sub>2</sub>O<sub>2</sub> (Wang et al., 2015). The higher catalytic activity of crude-activated carbons is the result of their active sites which are rich in structural electrons at their surfaces, which could improve the efficiency of H<sub>2</sub>O<sub>2</sub> to more than 95%. The Fe added to the carbon catalyst could also produce that total carbon content (TOC) removal and m-cresol conversion reached a 30% and 95%, respectively, after 2,000 hr in a chemical wet peroxide oxidation (CWPO) process. The Fe/SAC catalyzed reaction also revealed a conversion rate of 90% m-cresol in 1,800 hr. 2-methyl-p-benzoquinone and short-chain carboxylic acids were considered to be the major products in this catalytic oxidation of m-cresol, which were detected by gas chromatography–mass spectrometry and then calculated by density functional theory.

This study evaluates the oxidative elimination of O-cresol

in aqueous solution using local sodium clay (Mont-Na), in the presence of hydrogen peroxide H<sub>2</sub>O<sub>2</sub> at moderate temperatures. Here, we attempt to show how the introduction of the hydrogen peroxide reagent on O-cresol supported by the clay modifies the properties of the latter, in particular its adsorption capacity in its oxidation capacity. The catalyst was characterized before and after oxidation by X-ray diffraction, X-ray fluorescence, Fourier transform infrared spectroscopy, N<sub>2</sub> adsorption–desorption isotherm, chemical composition, pH at point of zero charge, and thermogravimetry coupled to mass spectroscopy (TGA/DTA-MS).

## Methodology

### Experimental protocol

Aqueous solutions of O-cresol were prepared by dissolving a known mass of O-cresol with deionized water in volumetric flasks. The stock solutions were stored in the dark at room temperature and then diluted to the desired concentrations. The oxidation experiments were conducted in batch mode using a multistation stirrer device (Memmert IPP200-500, 9 stations) with thermostatic bath (temperature controlled) with a regulated horizontal oscillation (300 cps/min). In a typical experiment, 15 mg of Mont-Na (commercial sodium clay of Montmorillonite type (Mont-Na) is provided by ENOF Company, National Company of the Non-ferrous Mining Products, Algeria) is suspended in a volume of 250 ml of a solution of O-cresol (62.5 mg/L) and H<sub>2</sub>O<sub>2</sub> (23.3 mM) (Herbache et al., 2016). However, different H<sub>2</sub>O<sub>2</sub> concentrations have been studied and an experiment without clay was also analyzed. The contact time is modified from 0 to 135 min. After such time, the liquid phase is recovered and filtered, and the concentration of O-cresol in aqueous phase was determined by UV–Vis at  $\lambda_{\max} = 270$  nm. The presence of different intermediates has been elucidated using also UV–Vis. The pH of this eluate is measured using CRISON micro pH 2001 device. The main parameters determined during the catalytic tests are thus pH, the O-cresol concentrations, intermediates, and in H<sub>2</sub>O<sub>2</sub>. The experimental tests of O-cresol adsorption over Mont-Na were carried out in previous work (Herbache et al., 2016). The conversion of O-cresol is calculated using the following equation:

$$\% \text{ Conversion} = (C_i - C_{eq}) * 100 / C_i$$

where  $C_i$  is the initial concentration of O-cresol (mg/L), and  $C_{eq}$  is its equilibrium concentration, which is determined at the end of the selected contact time (mg/L).

### **Characterization of the catalyst (Mont-Na)**

#### **X-ray fluorescence (XRF).**

X-ray fluorescence (XRF) analysis measurements of the elemental compositions of catalyst (clay) before and after oxidation were obtained using an automatic sequential wavelength dispersive X ray fluorescence spectrometer PW 2400 (Philips). Around 100 mg of samples was employed in order to deliver representative results.

#### **X-ray diffraction (XRD).**

The X-ray diffraction analyses of the samples were made using a Bruker D8-Advance diffractometer operating at the copper  $K\alpha$  wavelength ( $\lambda = 1.5406$ ) at a voltage of 20–60 kV and an intensity of 5–80 mA.

#### **FT infrared spectroscopy.**

Fourier transform infrared spectroscopy (FTIR) was performed using a Bruker Alpha spectrophotometer over a range of 350–3,800  $\text{cm}^{-1}$  with a resolution of 1  $\text{cm}^{-1}$ .

#### **Thermogravimetric analysis coupled with mass spectrometry:**

Temperature programmed desorption (TPD) experiments were performed in a TG-TDA equipment (Mettler Toledo, TGA/SDTA851e/LF/1600) coupled to a mass spectrometer (Pfeiffer Vacuum, THERMOSTAR GSD301T). The thermobalance was purged for 2 hr using a helium flow rate of 100 ml/min before the TPD running, and then heated up to 950°C (heating rate 20°C/min) while keeping the inert atmosphere.

#### **Specific surface ( $S_{\text{BET}}$ ) and point of zero charge $\text{pH}_{\text{pzc}}$ .**

The specific surface area of the adsorbents was determined by nitrogen physisorption at 77 K, using a Micromeritics ASAP 2000 volumetric adsorption device. The specific surfaces ( $S_{\text{BET}}$ ) of the adsorbent before and after adsorption and in the presence or absence of  $\text{H}_2\text{O}_2$  were calculated using the BET (Brunauer–Emmett– Teller) equation assuming that the surface of the nitrogen molecule is 16.2  $\text{\AA}^2$ . The microporous volumes and the pore width are calculated by applying the methods of Dubinin– Radushkevich (DR) and Barrett, Joyner, and Halenda (BJH) to the  $\text{N}_2$  adsorption–desorption isotherms. The point of zero charges  $\text{pH}_{\text{PZC}}$  has been estimated according to previous work (Herbache et al., 2016).

#### **UV-visible spectrophotometry.**

The concentration of targeted compounds during the catalytic oxidation kinetic tests was followed by UV-visible spectrophotometry using a brand Perkin-Elmer spectrophotometer (model Lambda 45) dual beam, operating over a range of 190–1,100 nm. The wavelength of the absorption maxima of O-Cresol is  $\lambda_{\text{max}} = 270$  nm and that of



2-methylbenzoquinone  $\lambda_{\text{max}} = 250 \text{ nm}$ .

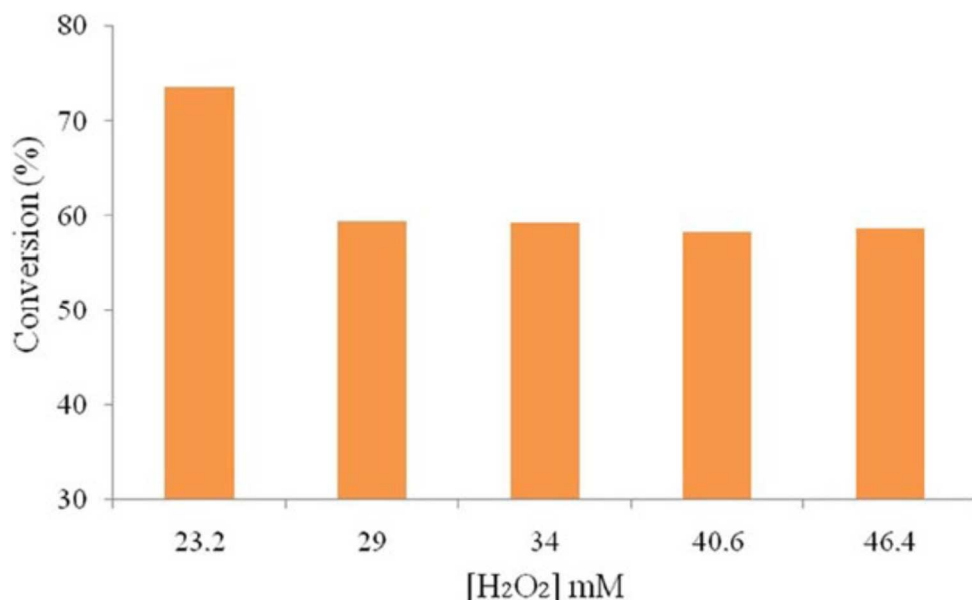


**Figure 1.** Effect of the initial H<sub>2</sub>O<sub>2</sub> concentration on the O-cresol degradation. [O-cresol]: 62.5 mg/L. Catalyst weight: 15 mg. Temperature: 25°C. pH = 7, Contact time: 150 min.

## Results and discussion

### Effect of H<sub>2</sub>O<sub>2</sub> addition

In order to determine the effect of H<sub>2</sub>O<sub>2</sub> reagent addition on catalytic oxidation, tests were carried out in the presence of the catalyst at different concentrations of H<sub>2</sub>O<sub>2</sub> at a temperature of 25°C.

The results compiled in Figure 1 show that the conversion of O-cresol decreases with H<sub>2</sub>O<sub>2</sub> concentration. Therefore, the maximum removal of the pollutant was achieved at the lowest H<sub>2</sub>O<sub>2</sub> concentration, 23.2 mM, where the oxidation yield of O-cresol was 73.6%. This hydrogen peroxide concentration has been fixed for the remaining oxidation tests. This correlates well with the results obtained from previous studies (Ling et al., 2015; Navalon et al., 2010; Yan et al., 2016), who studied in their works that adding H<sub>2</sub>O<sub>2</sub> promoted catalytic oxidation process, the degradation rate of phenolic compounds was obviously increased and involves the generation and subsequent reaction of hydroxyl radicals (OH•). Maximum degradation efficiency was attained at 31.64 mM. Moreover, addition of peroxide hydrogen affects the degradation efficiency, this due to self-decomposition of H<sub>2</sub>O<sub>2</sub>.

### Effect of temperature

Figure 2 shows that the temperature has a major effect on the process of oxidation. It clearly increases the degradation of the pollutant owing to the decomposition of hydrogen peroxide in the presence of catalyst into free radicals (Kavitha & Palanivelu, 2005; Khaki et al., 2017; Yan et al., 2016; Zaviska et al., 2009). In order to observe more clearly the effect of temperature, the conversion of O-cresol for a fixed time has been compared at different temperatures, Figure 2.

Indeed, when the temperature of the reaction increases from 25 to 55°C, the conversion rate of O-cresol increases from 73.6% to 84.6%. Similar findings are reported by different authors (Kurian & Sugunan, 2006; Lahbabi et al., 2009).

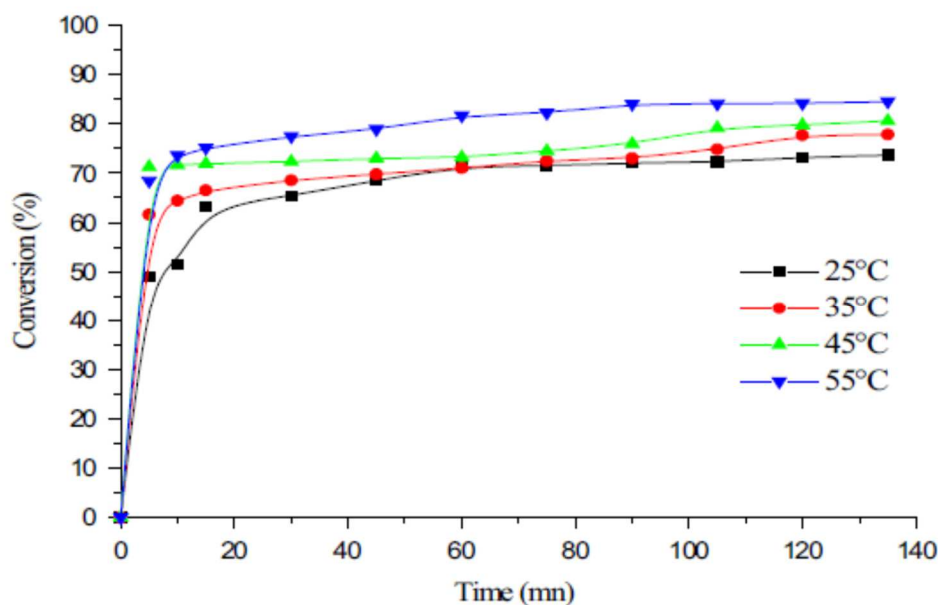


**Figure 2.** Effect of temperature on the catalytic oxidation of O-cresol. [O-cresol]: 62.5 mg/L. [H<sub>2</sub>O<sub>2</sub>] = 23.2 Mm. Catalyst weight: 15 mg. pH = 7. Contact time: 150 min.

### Effect of contact time

The kinetics of the catalytic oxidation of O-cresol with H<sub>2</sub>O<sub>2</sub> in the presence of clay has been analyzed in order to determine the time required for achieving the maximum oxidation. For this purpose, the conversion of O-cresol was monitored at different temperatures (25°, 35°, 45°, and 55°) with time. Figure 3 shows the conversion of O-cresol as a function of the reaction time. In the absence of catalyst, blank experiments indicated the absence of any significant degradation of O-cresol. Contrarily, the presence of Mont-Na greatly increases the conversion of the phenol compound. Thus, the catalytic oxidation process achieves O-cresol high conversions of more than 50% even 70% at 25°C and 55°C, respectively. Beyond this time, the conversion rate of O-cresol remains constant. From the curves obtained, the reaction time required for degradation of O-cresol to reach equilibrium of 84% at 55°C and 73% at different temperatures is up to 90 and 120 min, respectively. It has been shown in many researches that time has a promotional effect on the degradation of phenolic compounds. The catalytic performances of iron aluminum mixed pillared Montmorillonite and mesoporous material Fe<sub>2</sub>O<sub>3</sub>/MCM-41 toward hydroxylation of phenol with H<sub>2</sub>O<sub>2</sub> (Kurian & Sugunan, 2006; Yan et al., 2016).



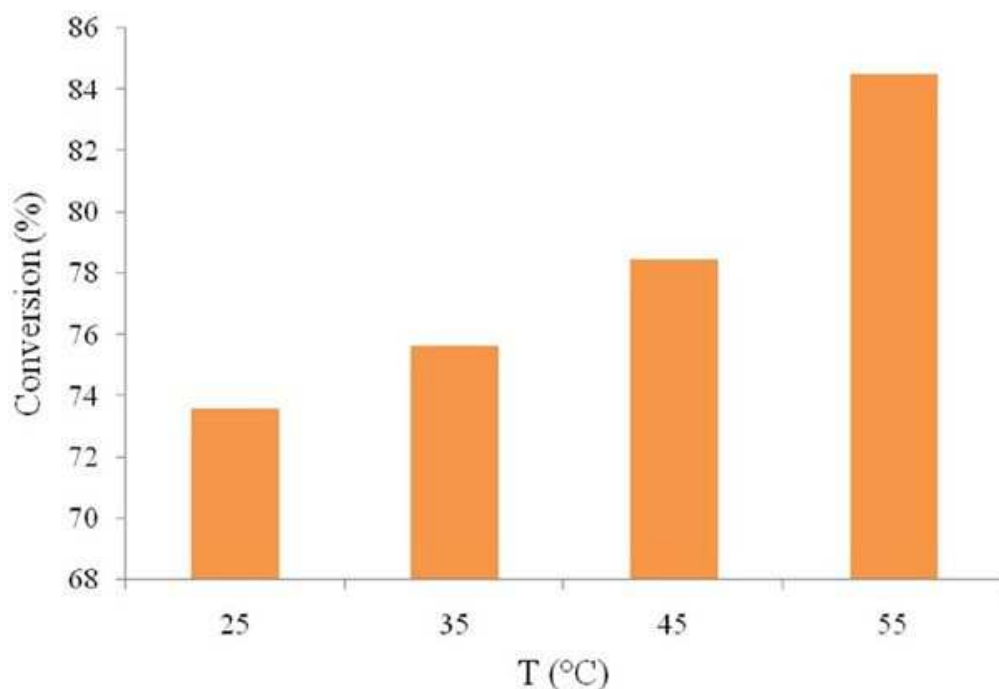


**Figure 3.** Kinetics of the catalytic oxidation of O-cresol at different temperatures. The evolution of the conversion is plotted as a function of the reaction time. [O-cresol]: 62.5 mg/L. [H<sub>2</sub>O<sub>2</sub>]: 23.2 mM. Catalyst weight: 15 mg. pH = 7.

### Effect of pH

From the results of Figure 4, it has been found that the degraded amount of O-cresol is greater and favored in a strongly acidic medium pH = 2 for all temperatures studied. It gradually decreased when the solution became neutral and basic.

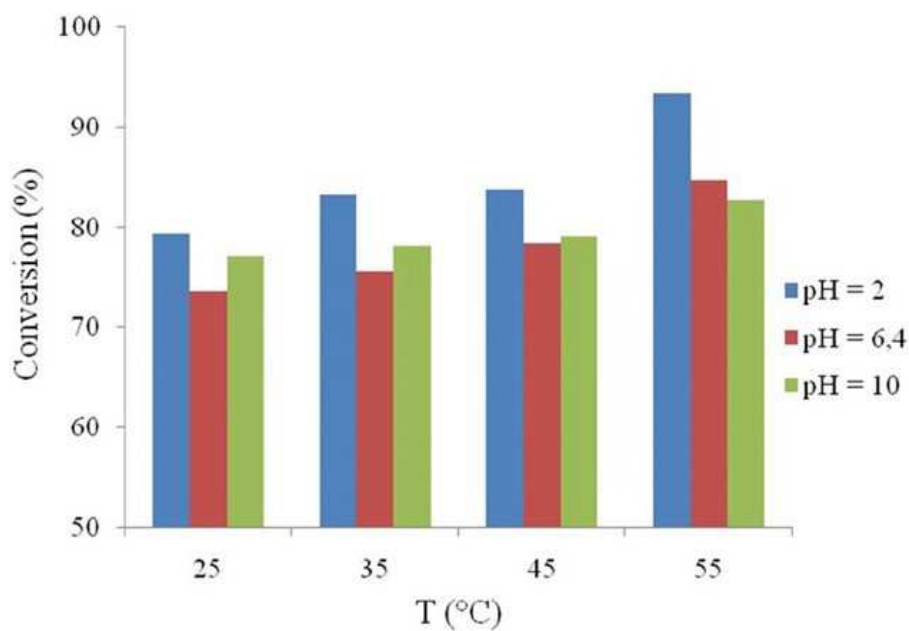
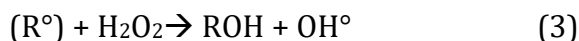
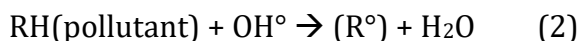
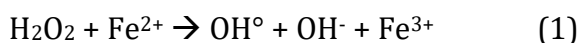


**Figure 4.** Effect of pH on the catalytic oxidation of O-cresol. [O-cresol]: 62.5 mg/L. [H<sub>2</sub>O<sub>2</sub>] = 23.2 Mm. Catalyst weight: 15 mg. Contact time: 150 min.

These results can be interpreted as follows:

- i) On the one hand, the oxidation depends on the nature of charges of the catalyst sites and the behavior of the oxidant  $\text{H}_2\text{O}_2$  according to the  $\text{pH}_{\text{pzc}}$  value of Mont-Na, which is = 5.11. At pH below  $\text{pH}_{\text{pzc}}$  (pH = 2), catalytic oxidation is favored by increasing the number of positive charges of the reactive ( $\text{H}^+$ ) sites of the catalyst (clay) that react with the oxidant  $\text{H}_2\text{O}_2/\text{Fe}^{2+}$  contained in the Mont-Na to produce free radicals ( $\text{HO}^\bullet$ ) in situ.
- ii) On the other hand, at  $\text{pH}_{\text{pzc}} > 5.11$  and therefore at neutral and basic pH (7 and 10), there would be an increase in the number of negative charges of active sites ( $\text{OH}^-$ ). Thus, the surface of Mont-Na becomes negatively charged, and consequently, the conversion rate of O-cresol decreases probably due to the electrostatic interaction of  $\text{Fe}^{2+}$  with  $\text{OH}^-$ . Moreover, the redox potential of  $\text{H}_2\text{O}_2$  decreases when the pH increases.

Indeed, it is shown in the literature that the decomposition of hydrogen peroxide ( $\text{H}_2\text{O}_2$ ) by iron generates radical species ( $\text{HO}^\bullet$ ) that are highly reactive with respect to organic molecules. This reaction is called the Fenton process. The catalytic oxidation reactions and in particular the decomposition of  $\text{H}_2\text{O}_2$  by the ferrous ions are presented as follows (Kavitha & Palanivelu, 2005; Wang et al., 2015; Zaviska et al., 2009):



In a very acidic medium (pH = 2), this mechanism is favored by the increase of the  $\text{H}_2\text{O}_2/\text{Fe}^{2+}$  ratio (Zaviska et al., 2009). On the other hand, at neutral and basic pH, iron ( $\text{Fe}^{2+}$  and  $\text{Fe}^{3+}$ ) is able to precipitate and form iron hydroxides, thus leading to a slight decrease in catalytic activity (Ellias & Sugunan, 2014; Kavitha & Palanivelu, 2005; Kurian & Sugunan, 2006; Molina et al., 2006; Wang et al., 2015; Zaviska et al., 2009). Our results seem to be in agreement with this mechanism. Thus, in Table 1, the reduction of the iron content after the catalytic oxidation shows that the oxidation process has taken place. This correlates well with the results interpreted previously.

Table 1. Mont-Na fluorescence X before and after catalytic oxidation

Element (%)	O	Si	Al	Mg	K	Fe	Na
Mont-Na	48.9	29.9	12.5	1.94	0.87	2.04	3.29
Mont-AO	49.6	32.9	9.85	2.18	1.66	1.62	1.38

The free radicals  $\text{OH}^\bullet$  have a very marked electrophilic character, and organic compounds with electron donor groups react more rapidly with them, leading to the formation of ortho- or para-hydroxylated intermediates via an electrophilic reaction (Zaviska et al., 2009). Several studies

have been made for the catalytic oxidation of phenol and cresols (Adan et al., 2009; Khunphonoi & Grisdanurak, 2016; Valsania, Fasano, Richardson, & Vincenti, 2012; Wang et al., 2015; Zaviska et al., 2009), and have allowed to identify the formation of pyrocatechol, hydroquinone, and benzoquinone. Indeed, the degradation of O-cresol in by-products is similar to that of phenol. The di-hydroxylated products (biphenols) are in turn attacked by the free radicals  $\text{OH}^\bullet$  leading to the opening of the aromatic ring, forming carboxylic acids and finally the  $\text{H}_2\text{O}$  and  $\text{CO}_2$ .

Also, the representation of the absorbance of the disappearance of O-cresol ( $\lambda_{\text{max}} = 270$  nm) as a function of time (Figure 5) confirms these results. In it, the by-product formation is observed: 2-methylbenzoquinone ( $\lambda_{\text{max}} = 250$  nm) following degradation of O-cresol. A yield of more than 84.6% degradation of o-cresol is obtained after 80 min of reaction time at a temperature of 55°C. The final absorbance values of cresol and 2-methylbenzoquinone decrease considerably. These results show that O-cresol is completely degraded and that 2-methylbenzoquinone is transformed into other by-products.

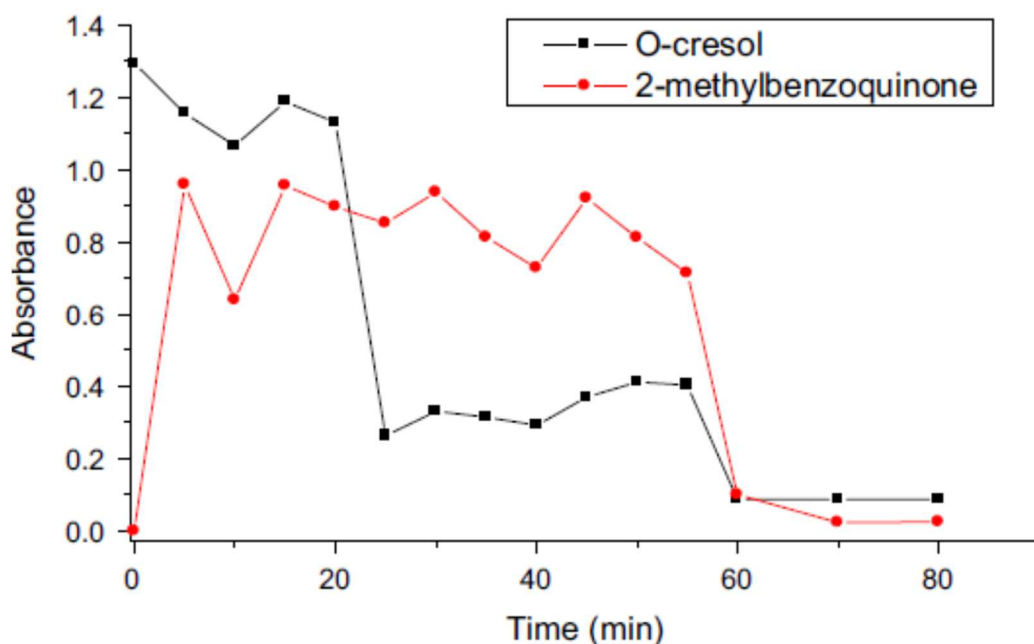


**Figure 5.** Evolution of the degradation of O-cresol and the formation of 2-methylbenzoquinone as a function of the reaction time (O-Cresol  $\lambda_{\text{max}} = 270$  nm, 2-methylbenzoquinone  $\lambda_{\text{max}} = 250$  nm). [O-cresol]: 62.5 mg/L. [ $\text{H}_2\text{O}_2$ ]: 23.2 mM. Catalyst weight: 60 mg.

Figure 6 shows the evolution of the pH of the medium during the oxidation of O-cresol. The rapid pH decreases from 6.4 to 4.5 proves that there is formation of 2-methylbenzoquinone and methylhydroquinone after 5 min of oxidation. Indeed, hydroquinones and benzoquinones are di-acids whose pH is between 4 and 4.7. The next oxidation step is the opening of the benzene ring, leading to the formation of carboxylic acids, which justifies the low pH values observed after 5 min (Figure 6). After such time, the pH value increases and reaches a neutral value after 60 min of oxidation. This would be a proof that the carboxylic acids are being degraded to  $\text{H}_2\text{O}$  and  $\text{CO}_2$  in the later stages of the treatment.

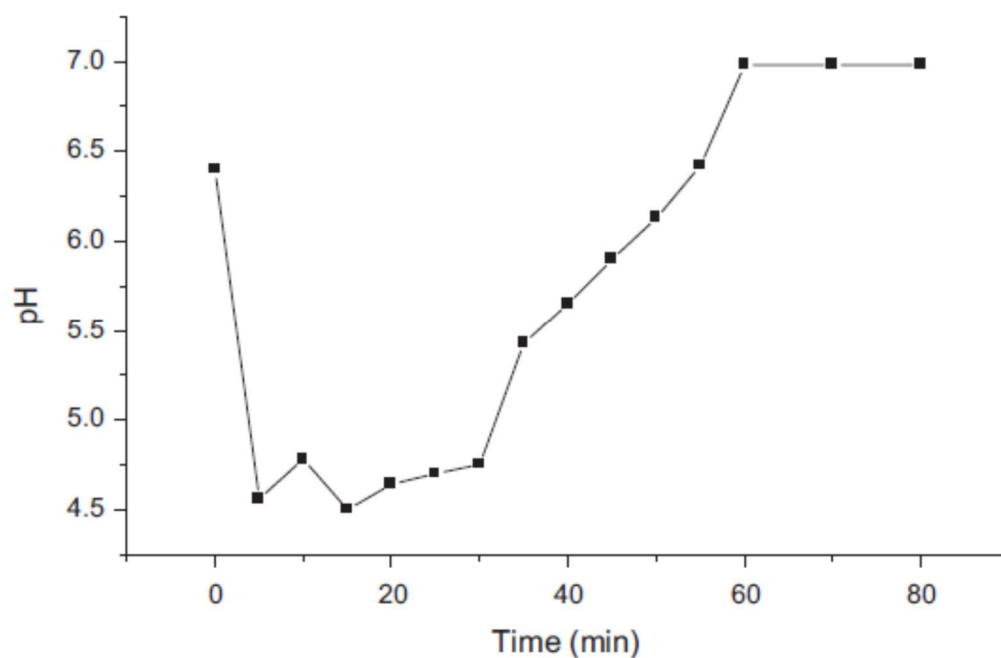


Figure 6. Evolution of the pH of the reaction medium during the catalytic degradation of O-cresol supported by Mont-Na. [O-cresol]: 62.5 mg/L. [H<sub>2</sub>O<sub>2</sub>]: 23.2 mM. Catalyst weight: 60 mg.

Figure 7 presents a possible degradation scheme for the O-cresol oxidation process taking place in the presence of Mont-Na (Figures 6, 7).

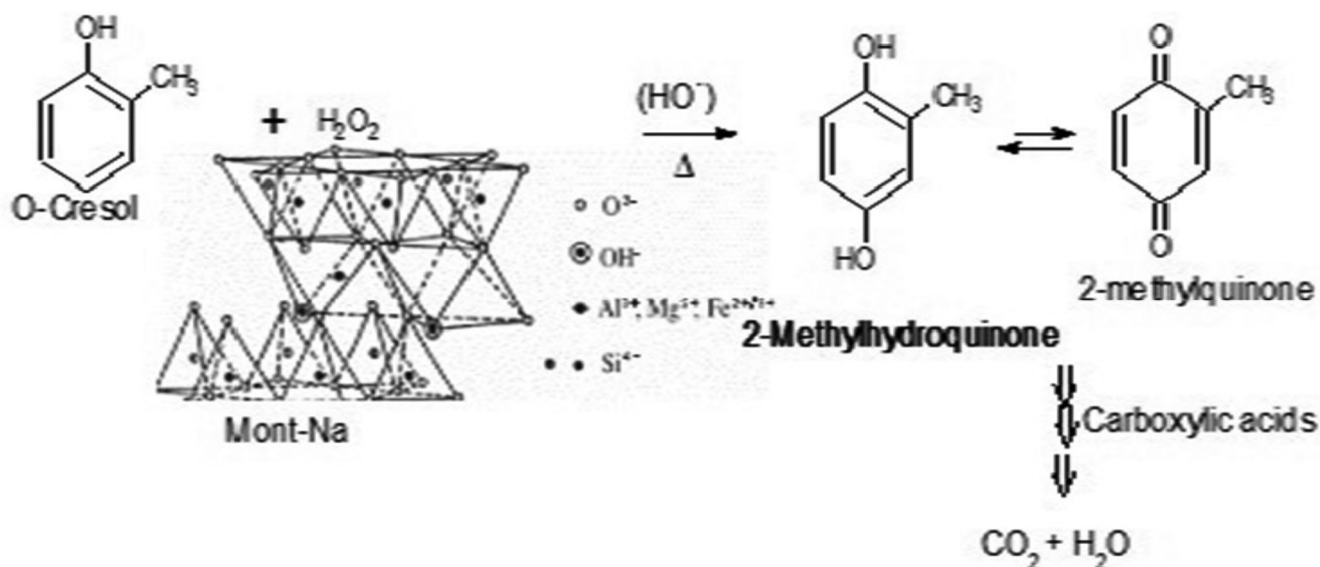


Figure 7. Catalytic oxidation of O-Cresol supported by Mont-Na.

There have been numerous references in the literature to investigate the cresol degradation mechanism by other oxidation process: ozonation, electrochemical oxidation, and photocatalytic oxidation etc....Several highly hydrophilic degradation intermediates have been identified (Valsania et al., 2012) for cresols. The ozonation reaction mechanism assumed is subdivided into three steps, involving the ring opening of the phenolic group, followed by the formation of several by-products intermediates in the increasing oxidation state. This leads subsequently to the formation of relatively stable products, such as carboxylic acids (malonic and oxalic). The electrochemical behavior of cresol on platinum electrodes has been studied using cyclic voltammetry and in situ FTIR spectroscopy (Taleb, Montilla, Quijada, Morallon, & Taleb, 2014). From the results, it can be concluded that the main soluble products formed during the oxidation of O-cresol in acid medium are CO<sub>2</sub> and methyl-p-benzoquinone.

Abdollahi, Abdullah, Zainal, and Yusof (2011) studied the degradation of O-cresol in the presence of UV; by ZnO as photocatalyst. The results showed that the photodegradation of O-cresol leads to the formation of the intermediates: 2-methylresorcinol and 2,5-hydroxybenzaldehyde, and may be the presence of carboxylic acids.

### **X-ray fluorescence**

Table 1 shows the XRF analysis of the Mont-Na before and after the catalytic oxidation. The analysis has been repeated again on a sample recovered after the catalytic oxidation test at 55°C. The presence of oxygen (O) and silicon (Si) in a substantial amount, and of aluminum (Al) and iron (Fe) in a lower extend, is expected owing to the well-known composition of Mont-Na. After the catalytic tests are completed, it can be seen that Fe and Al levels are lowered from 2.04% to 1.62% and 12.5% to 9.85%, respectively. Also, an increase in O content from 48.9% to 49.6% was observed.

The quantitative elemental analysis of Mont-Na catalysts has been performed by means of X-ray fluorescence, and the results are presented in Table 1. It can be observed that the clay contains a high amount of iron that could participate in the mechanism of oxidation of O-cresol. Then, the introduction of H<sub>2</sub>O<sub>2</sub> could improve the oxidation of this compound by the formation of radicals as the well-known Fenton mechanism, because in the absence of clay, any significant degradation of O-cresol is produced.

### **X-ray diffraction (XRD)**

X-ray diffraction was performed for three samples: Mont-Na local clay before and after adsorption (Mont-A) and also after catalytic oxidation of O-cresol (Mont-AO). The initial XRD profile shows the lines corresponding to Montmorillonite and Illite. Examination of the local Mont-Na clay diffractogram (Figure 8) indicates a lattice distance of 12.6 Å. It should be noted that both the adsorption and the catalytic oxidation of O-cresol have undergone significant changes in Mont-Na structure, as pointed out by the slight decrease in the intensity of the signal collected and the shifting of the characteristic peaks of Montmorillonite. The diffractogram of Mont-A shows an increase of d<sub>001</sub> from 12.6 to 14.5 Å. This variation is

due to the presence of O-cresol molecules incorporated in the interfoliar space during adsorption. The diffractogram of the local clay in the presence of the oxidant  $\text{H}_2\text{O}_2$  shows an increase in the basal area of the Mont-Na sample. Thus, the peak at  $12.6 \text{ \AA}$  of the (001) sample line (Mont-OA) widens and reaches a maximum of  $15.2 \text{ \AA}$  over that of the Mont-A sample. This is due to the hydration of the catalyst by the water molecules formed during the oxidation to more than 84% cresol, the rest being incorporated into the interfoliar space. In addition, the height of all Montmorillonite peaks decreases ( $2\theta = 20.6^\circ, 21.5^\circ, 23.1^\circ, 27^\circ, 43^\circ$ ). The height of all the Illite peaks decreases ( $2\theta = 14.90^\circ, 20.70^\circ, \text{ and } 29.36^\circ$ ).

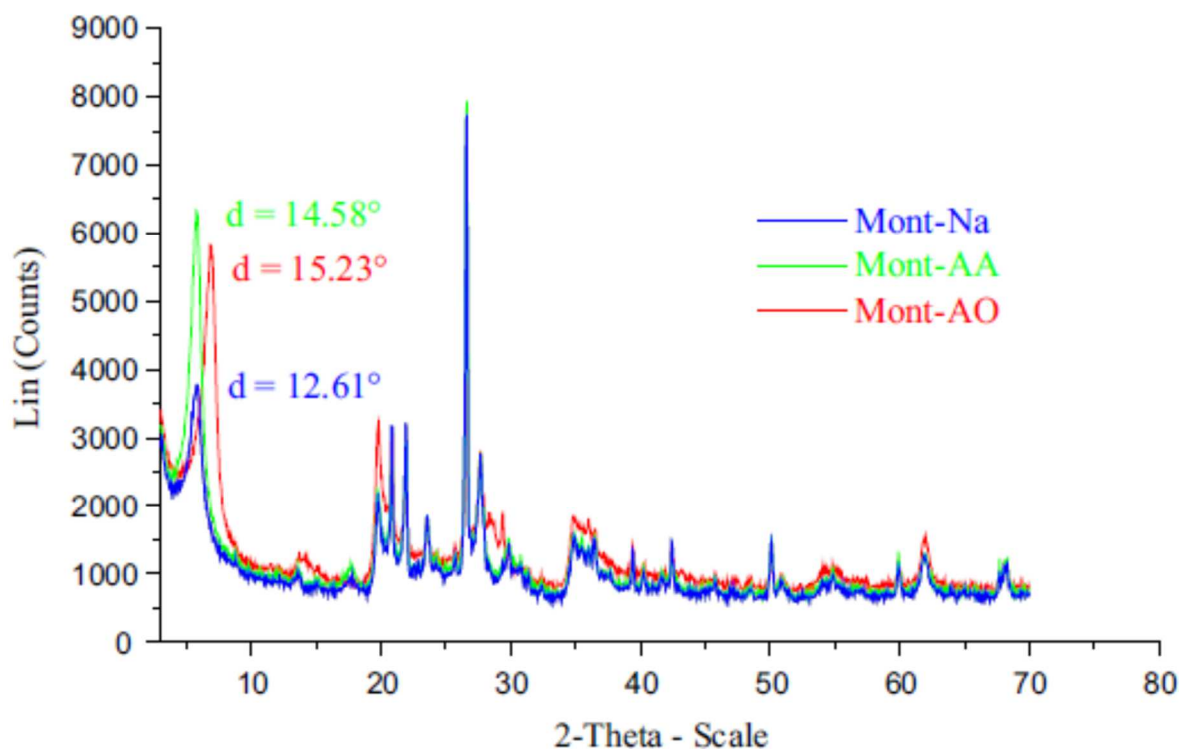


**Figure 8.** X-ray diffractogram of Mont-Na, Mont-A, and Mont-AO samples.

### Infrared spectroscopy

Changes in the surface chemistry of Mont-Na after adsorption and oxidation experiments have been analyzed by means of FTIR, being reported in Figure 9. The disappearance of certain bands in the spectra of the samples is noted. This is the case for Mont-A and Mont-AO samples, where the peak located at  $1,464 \text{ cm}^{-1}$  in Mont-Na, characteristic of carbonates, is no longer seen, pointing out the disappearance of impurities (Herbache et al., 2016; Madejova, 2003). The band located between  $3,200$  and  $3,750 \text{ cm}^{-1}$ , with a shoulder at  $3,622 \text{ cm}^{-1}$  characterizing Montmorillonite, corresponds to the elongation vibrations of the OH groups of the octahedral layer (Madejova, 2003). As for the OH bands, the comparison between the three spectra reveals a decrease and an increase are recorded in the intensity of stretching vibration bands of OH groups. They are centered at  $1,634 \text{ cm}^{-1}$ , for the Mont-A and Mont-AO samples following the



catalytic oxidation of O-cresol. They are also associated with the OH groups of the water constitution and the water adsorbed between the sheets. In addition, a large observed widening of the band corresponds to the elongation vibrations of the OH groups of the octahedral layer for Mont-OA situated around 3,200–3,750  $\text{cm}^{-1}$ .

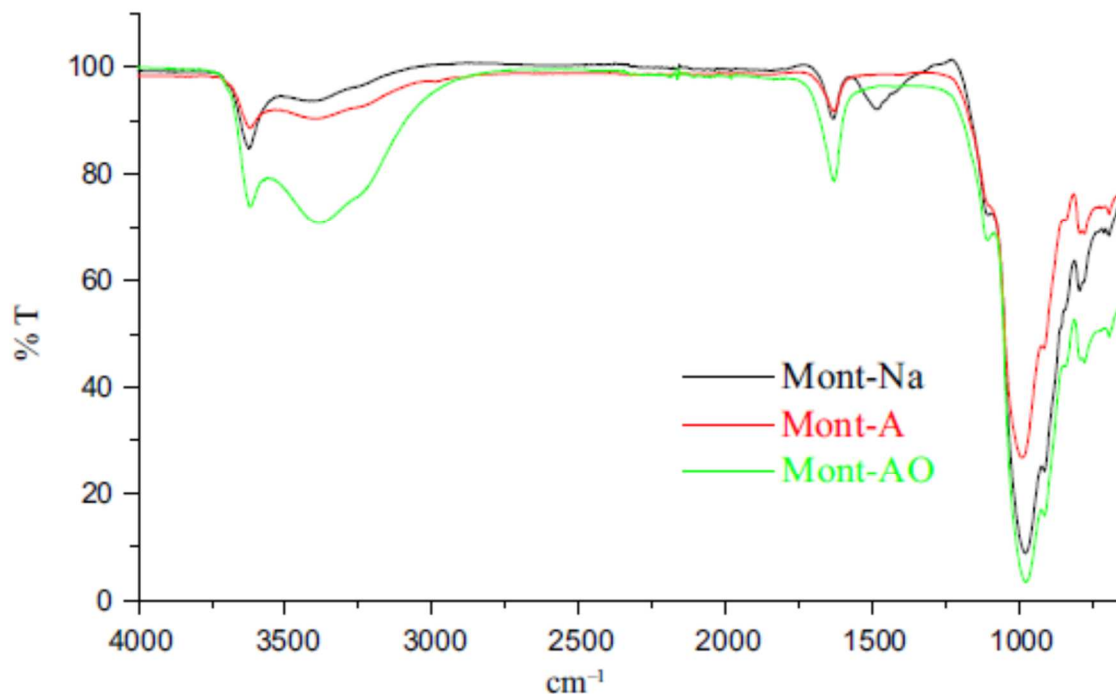


**Figure 9.** FTIR spectra of Mont-Na, Mont-A, and Mont-AO samples.

### Textural properties

The porosity of Mont-Na has been determined from the  $\text{N}_2$  adsorption–desorption isotherms before and after the O-cresol adsorption and oxidation experiments. Table 2 compiles the most important textural parameters that are calculated from the  $\text{N}_2$  adsorption isotherms. Mont-Na shows a type IV porous isotherm, characteristic of mesoporous solids. Surface area as determined from BET method starts at 67  $\text{m}^2/\text{g}$  for Mont-Na. This value decreases to 43  $\text{m}^2/\text{g}$  after adsorption of O-cresol (Mont-A sample in Table 1). This is related to the existence of O-cresol molecules inserted into the interlaminar space. Interestingly, the reduction of the specific surface area is even larger for the Mont-AO sample (40  $\text{m}^2/\text{g}$ ) when compared to the surface of the Mont-A sample. However, the micropore volume increases after the adsorption and oxidation experiments, Table 2. This can be related to the removal of impurities, such as carbonates, which have been already documented in the FTIR results.

**Table 2.** BET-specific surface area values of Mont-Na before and after adsorption and oxidation of O-cresol experiments

Samples	MONT-NA	MONT-A	MONT-AO
$S_{\text{BET}}$ ( $\text{m}^2/\text{g}$ )	67	43	40
Volume of micropores ( $\text{cm}^3/\text{g}$ )	0.04	0.08	0.06
Pore diameter ( $\text{\AA}$ )	406	547	510

### Thermogravimetric analysis coupled with mass spectrometry

Three (03) stages of dehydration (elimination of water), endo-thermic process characterizes the sodium clay: Mont-Na, Figure 10. The first step corresponds to the removal of hygroscopic water (starting water molecules free of hydration) at a temperature  $< 100^\circ\text{C}$ . The second corresponds to the loss of weight associated with the desorption of the water adsorbed in the interfoliar space at a temperature of  $450^\circ\text{C}$ . The last step corresponds to the elimination of the water constitution of the clay (dehydroxylation of the sheets ( $\text{OH}^-$  of the structure of clays (crystalline water) at the temperature of  $600^\circ\text{C}$ )).

So, the weight loss is 2.5% of free water molecules of hydration between  $50$  and  $90^\circ\text{C}$ . 2.0% for the water adsorbed in the interfoliar space at  $400^\circ\text{C}$ . Finally, the loss in weight is 13% for the water associated with the dehydroxylation of the sheets (crystalline water) (Mohan & Pittman, 2007; Ourari, Tennah, Ruíz-Rosas, Aggoun, & Morallón, 2018), toward  $600^\circ\text{C}$ .

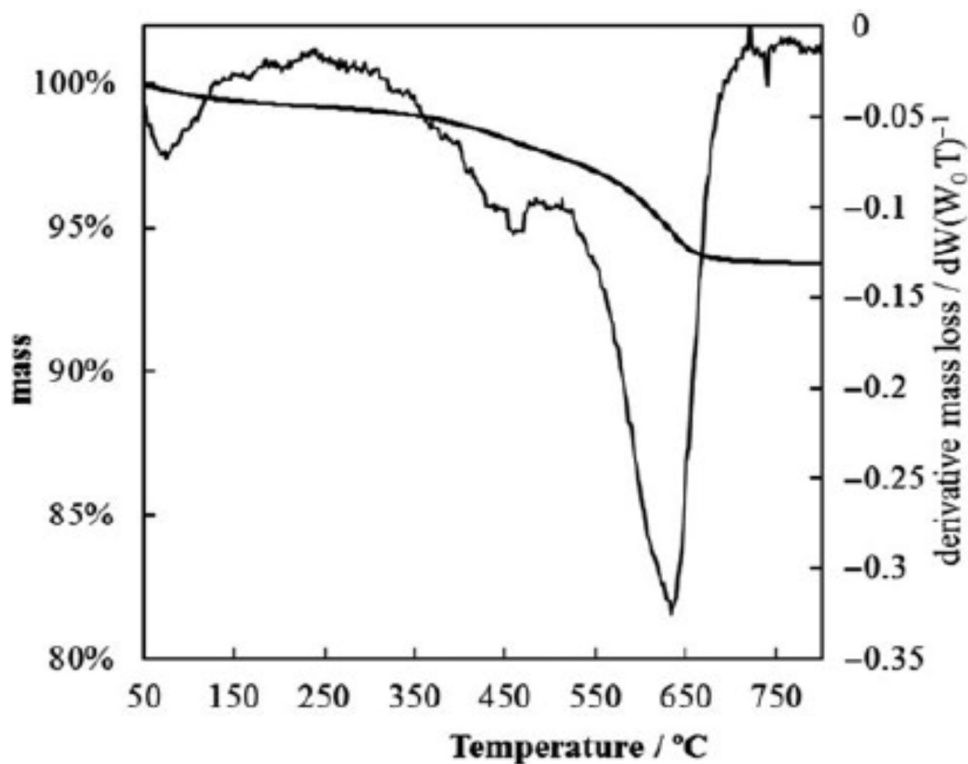


**Figure 10.** Thermogravimetric analysis of Mont-Na sample.

In Figure 11, the thermogravimetric profile of O-cresol/ Mont-Na adsorption has four endothermic stages, three of which correspond to the desorption of the three different types of water discussed above and whose quantities have changed. 7.5% of free water molecules of hydration are desorbed in the first step. Between 100 and 150°C, the desorption of O-cresol is 13%. A loss in weight of 2.0% of the water adsorbed in the interfoliar space at 400°C and a loss in weight of 4% of the water associated with the dehydroxylation of the sheets ( $\text{OH}^-$  of the structure of the clays (Mohan & Pittman, 2007), toward 600°C).

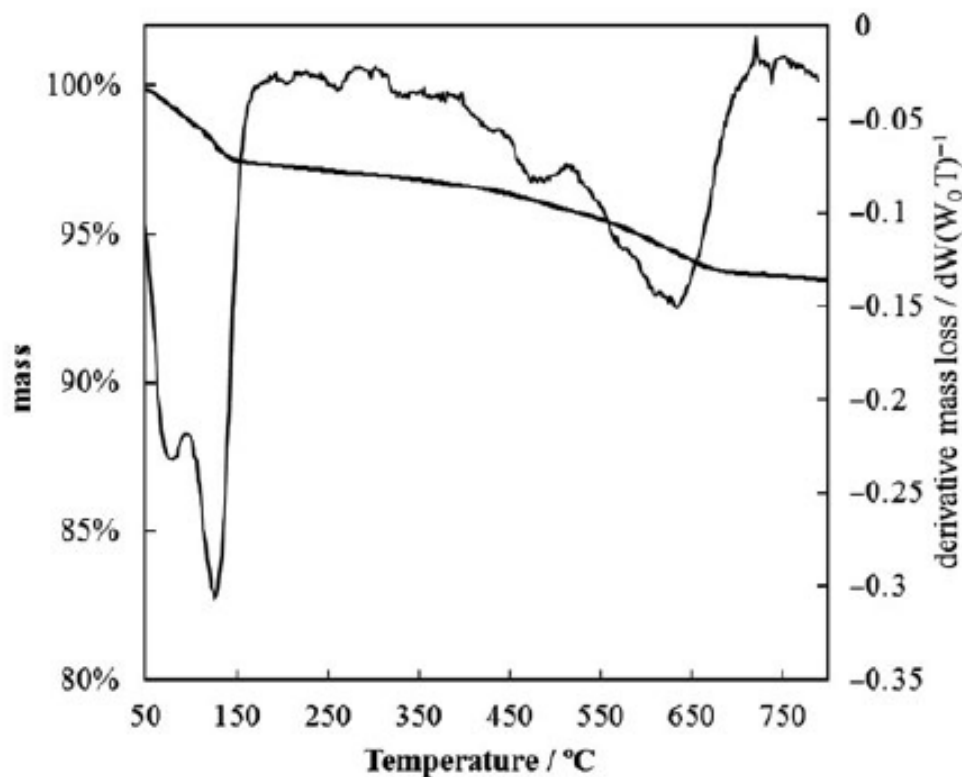


**Figure 11.** Thermogravimetric analysis of the Mont-Na sample after O-cresol adsorption.

For the oxidation of O-cresol-Mont-Na, Figure 12, there are also four endothermic stages, three of which correspond to the loss of the three different types of water discussed above and whose quantities have changed. The weight of the remaining O-cresol is 4%, and weight loss of free water molecules and the water of the interfoliar space is 13% and 0.5%, respectively. Finally, a loss in weight of 4% of the crystalline water (Mohan & Pittman, 2007), toward 600°C, is observed.

It is important to note that the amount of desorbed water has increased during the oxidation reaction. Indeed, the mass loss (Figure 12) is 13% relative to the 7.5% mass loss (Figure 11) during the adsorption of cresol in the absence of  $\text{H}_2\text{O}_2$ . This could confirm the total oxidation of the pollutant by forming  $\text{H}_2\text{O}$  and  $\text{CO}_2$ . In addition, the DTA coupled to the MS allow us to confirm this degradation since in Figure 13, and under the atmosphere of inert gas (Helium), the presence

of CO<sub>2</sub> and H<sub>2</sub>O is noted. The presence of CO<sub>2</sub> would come from the decomposition of cresol. Mass spectroscopy does not detect the latter.

It should be noted that the peak of CO<sub>2</sub> is more intense under atmospheric air because of the presence of this gas in the air (Figure 13).

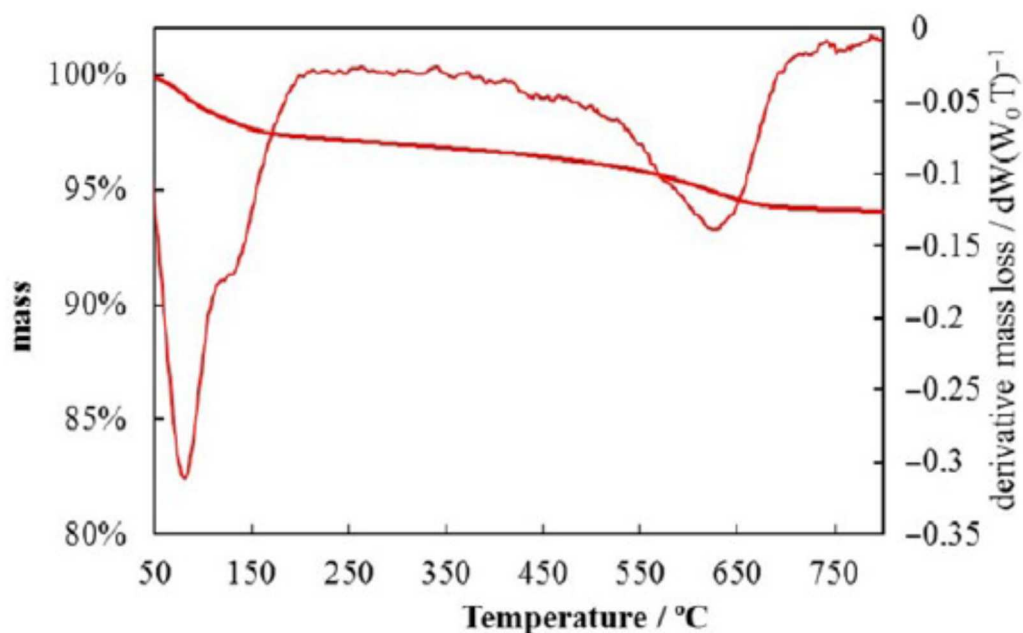


**Figure 12.** DTA/TGA profile of oxidation of O-cresol-Mont-Na.

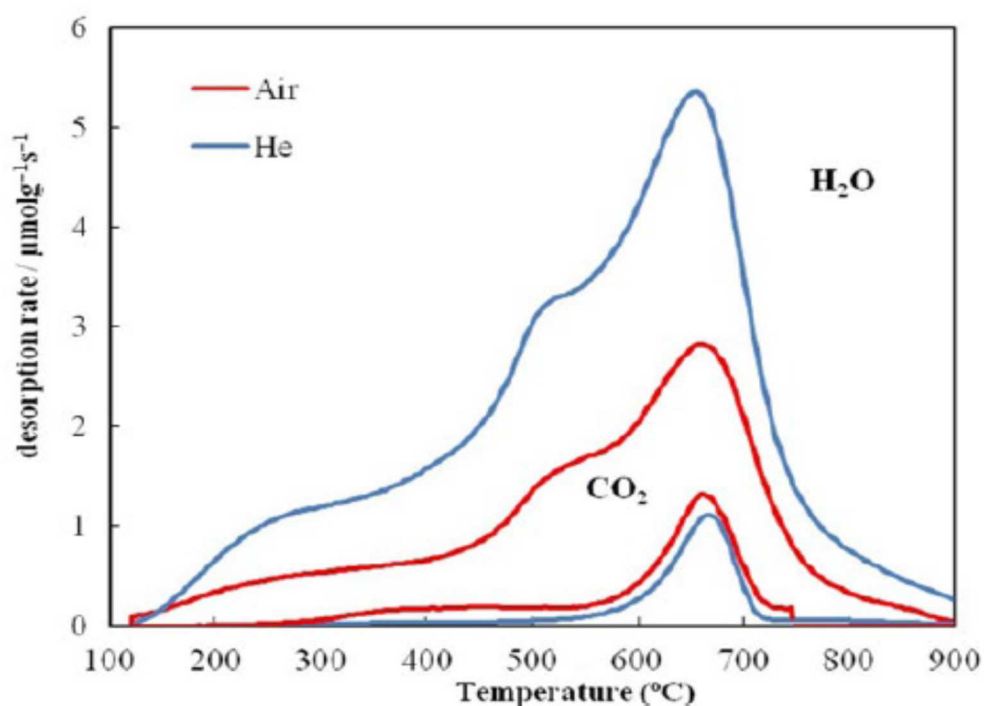


**Figure 13.** DTA/MS analysis of Mont-A and Mont-AO samples under atm He and atm air.

## Conclusions

In this work, the use of local clay shows a great potential for catalyst properties in the presence of the oxidizing reagent  $\text{H}_2\text{O}_2$  for the degradation of O-cresol. The effect of some experimental parameters has been studied using a batch oxidation technique. The major findings are as follows:

- The results showed that the degradation as well as the conversion rate of O-cresol is rapid where the equilibrium is reached after 90 min with a percentage of about 84.6% at a temperature of  $55^\circ\text{C}$  and  $[\text{H}_2\text{O}_2] = 23.2 \text{ mM}$ , then it remains constant.
- The influence of pH has shown that the O-cresol oxidation is favored in acidic medium. The degraded amount of O-cresol is greater in a strongly acidic medium  $\text{pH} = 2$  and then it gradually decreased when the solution became neutral and basic.
- The formation of 2-methylbenzoquinone increases at the same time as the rise in temperature.
- The decrease in the iron content and the increase in the oxygen content present in the catalyst after the catalytic oxidation show that the oxidation process has taken place.
- Moreover, the possible modifications of the structural, textural, and surface chemistry properties of Mont-Na have been analyzed before and after the catalytic test using several techniques (X-ray diffraction, Fourier transform infrared spectroscopy,  $\text{N}_2$  adsorption-desorption isotherm at 77 K, thermogravimetric analysis coupled to mass spectroscopy, chemical composition, and pH at point of zero charge).
- The set of characterization results suggests that this is a catalytic oxidation of O-cresol following degradation to other intermediate hydroxylated organic compounds such as carboxylic acids and the final products  $\text{H}_2\text{O}$  and  $\text{CO}_2$ .
- $\text{H}_2\text{O}_2$  oxidation of O-cresol in the presence of local clay proved to be an effective means for the removal and degradation of O-cresol contained in industrial influents.

## Acknowledgments

Financial support for this work by the Algerian Directorate General of Scientific Research and Technological Development (DGRSDT) and the Ministry for Higher Education and Scientific Research is gratefully appreciated. The authors would like to thank the staff of Servicios Técnicos de Investigación (SSTI) of the University of Alicante for performing characterization.

## REFERENCES

- Abdollahi, Y., Abdullah, A. H., Zainal, Z., & Yusof, N. A. (2011). Photodegradation of O-cresol by ZnO Under Visible Light Irradiation. *International Journal of Engineering Science & Advanced Technology*, 8(2), 135–144.
- Adan, C., Carbajo, J., Bahamonde, A., & Martinez-Aias, A. (2009). Phenol photodegradation with oxygen and hydrogen peroxide over TiO<sub>2</sub> and Fe-doped TiO<sub>2</sub>. *Catalysis Today*, 143(3–4), 247–252. <https://doi.org/10.1016/j.cattod.2008.10.003>
- Adav, S. S., Chen, M. Y., Lee, D. J., & Ren, N. Q. (2007). Degradation of phenol by aerobic granules and isolated yeast *Candida tropicalis*. *Biotechnology and Bioengineering*, 96(5), 844–852. [https://doi.org/10.1002/\(ISSN\)1097-0290](https://doi.org/10.1002/(ISSN)1097-0290)
- ATSDR. (2008) *Agency for Toxic Substances and Disease Registry Division of Toxicology and Health Human Sciences* (ATSDR), Cresols - ToxFAQs™, N° CAS 1319-77-33.
- Bertella, F., & Pergher, S. B. C. (2015). Pillaring of bentonite clay with Al and Co. *Microporous and Mesoporous Materials*, 201, 116–123. <https://doi.org/10.1016/j.micromeso.2014.09.013>
- Borji, S. H., Nasser, S., Mahvi, A. H., Nabizadeh, R., & Javadi, A. H. (2014). Investigation of photocatalytic degradation of phenol by Fe(III)-doped TiO<sub>2</sub> and TiO<sub>2</sub> nanoparticles. *Journal of Environmental Health Science and Engineering*, 12, 101–110. <https://doi.org/10.1186/2052-336X-12-101>
- Chen, D., Li, F., Zong, L., Sun, X., Zhang, X., Zhu, C., ... Li, A. (2016). Integrated adsorptive technique for efficient recovery of m-cresol and m-toluidine from actual acidic and salty wastewater. *Journal of Hazardous Materials*, 312, 192–199. <https://doi.org/10.1016/j.jhazmat.2016.03.056>
- Deng, Y., & Englehardt, J. D. (2006). Treatment of landfill leachate by the Fenton process. *Water Research*, 40(20), 3683–3694. <https://doi.org/10.1016/j.watres.2006.08.009>
- Ellias, N., & Sugunan, S. (2014). Wet peroxide oxidation of phenol over cerium impregnated aluminium and iron- aluminium pillared clays. *Journal of Applied Chemistry*, 7(5), 80–85.
- Feddal, I., Ramdani, A., Taleb, S., Gaigneaux, E. M., Batis, N., & Ghaffour, N. (2014). Adsorption capacity of methylene blue, an organic pollutant, by montmorillonite clay. *Desalination and Water Treatment*, 52(13–15), 2654–2661. <https://doi.org/10.1080/19443994.2013.865566>
- Gavrilescu, M., Demnerová, K., Amand, J., Agathos, S., & Fava, F. (2015). Emerging pollutants in the environment: Present and future challenges in biomonitoring, ecological risks and bioremediation. *New Biotechnology*, 32(1), 147–156. <https://doi.org/10.1016/j.nbt.2014.01.001>
- Gil, A., Korili, S. A., & Vicente, M. A. (2008). Recent advances in the control and characterization of the porous structure of pillared clay catalysts. *Catalysis Reviews*, 50(2), 153–221. <https://doi.org/10.1080/01614940802019383>
- Hadjar, H., Hamdi, B., & Ania, C. O. (2011). Adsorption of p-cresol on novel diatomite/ carbon composites. *Journal of Hazardous Materials*, 188(1–3), 304–310. <https://doi.org/10.1016/j.jhazmat.2011.01.108>
- Herbache, H., Ramdani, A., Maghni, A., Taleb, Z., Taleb, S., Morallon, E., & Brahmi, R. (2016). Removal



- of o-Cresol from aqueous solution using Algerian Na-Clay as adsorbent. *Desalination and Water Treatment*, 57(43), 20511–20519. <https://doi.org/10.1080/19443994.2015.1108240>
- Hernandez-Esparza, M., Doria-Serrano, M. C., Acero Salinas, G., & Ruiz-Trevino, F. A. (2006). Removal of high phenol concentrations with adapted activated sludge in suspended form and entrapped in calcium alginate/ poly (N-vinyl pyrrolidone) hydrogels. *Biotechnology Progress*, 22(6), 1552–1559.
- Hocine, O., Boufatit, M., & Khouider, A. (2004). Use of montmorillonite clays as adsorbents of hazardous pollutants. *Desalination*, 167(1), 141–145. <https://doi.org/10.1016/j.desal.2004.06.122>
- Huang, J. (2009). Treatment of phenol and p-cresol in aqueous solution by adsorption using a carbonylated polymeric adsorbent. *Journal of Hazardous Materials*, 168(2–3), 1028–1034. <https://doi.org/10.1016/j.jhazmat.2009.02.141>
- Jiang, S., Zhang, H., & Yan, Y. (2015). Catalytic wet peroxide oxidation of phenol wastewater over a novel Cu-ZSM-5 membrane catalyst. *Catalysis Communications*, 71, 28–31. <https://doi.org/10.1016/j.catcom.2015.08.006>
- Kausar, A., Iqbal, M., Javed, A., Aftab, K., Nazli, Z., Bhatti, H. N., & Nouren, S. (2018). Dyes adsorption using clay and modified clay: A review. *Journal of Molecular Liquids*, 256, 395–407. <https://doi.org/10.1016/j.molliq.2018.02.034>
- Kavitha, V., & Palanivelu, K. (2005). Destruction of cresols by Fenton oxidation process. *Water Research*, 39(13), 3062–3072. <https://doi.org/10.1016/j.watres.2005.05.011>
- Kennedy, L. J., Vijaya, J. J., Sekaran, G., & Kayalvizhi, K. (2007). Equilibrium, kinetic and thermodynamic studies on the adsorption of m-cresol onto micro- and mesoporous carbon. *Journal of Hazardous Materials*, 149(1), 134–143. <https://doi.org/10.1016/j.jhazmat.2007.03.061>
- Khaki, M. R. D., Shafeeyan, M. S., Raman, A. A. A., & Daud, W. M. A. W. (2017). Application of doped photocatalysts for organic pollutant degradation - A review. *Journal of Environmental Management*, 198(2), 78–94. <https://doi.org/10.1016/j.jenvman.2017.04.099>
- Khunphonoi, R., & Grisdanurak, N. (2016). Mechanism pathway and kinetics of p-cresol photocatalytic degradation over titania nanorods under UV-visible irradiation. *Chemical Engineering Journal*, 296, 420–427. <https://doi.org/10.1016/j.cej.2016.03.117>
- Kurian, M., & Sugunan, S. (2006). Wet peroxide oxidation of phenol over mixed pillared montmorillonites. *Chemical Engineering Journal*, 115(3), 139–146. <https://doi.org/10.1016/j.cej.2005.08.010>
- Lahbabi, N., Rais, Z., Hajjaji, M., & Kacim, S. (2009). Oxydation du phenol sur un catalyseur à base de Fer supporté sur une argile marocaine. *Afrique Science: Revue Internationale des Sciences et Technologie*, 5(3), 14–24.
- Lassouane, F., Amrani, S., & Aït-Amar, H. (2013). Evaluation of o-cresol degradation potential by a strain of *Pseudomonas aeruginosa* S8. *Desalination and Water Treatment*, 51(40–42), 7577–7585. <https://doi.org/10.1080/19443994.2013.776503>
- Li, Y., Hu, X., Liu, X., Zhang, Y., Zhao, Q., Ning, P., & Tian, S. (2018). Adsorption behavior of phenol by

- reversible surfactant-modified montmorillonite: Mechanism, thermo- dynamics, and regeneration. *Chemical Engineering Journal*, 334, 1214–1221. <https://doi.org/10.1016/j.cej.2017.09.140>
- Ling, H., Kim, K., Liu, Z., Shi, J., Zhu, X., & Huang, J. (2015). Photocatalytic degradation of phenol in water on as-prepared and surface modified TiO<sub>2</sub> nanoparticles. *Catalysis Today*, 258(1), 96–102. <https://doi.org/10.1016/j.cattod.2015.03.048>
- Madejova, J. (2003). FTIR techniques in clay mineral studies review. *Vibrational Spectroscopy*, 31(1), 1–10. [https://doi.org/10.1016/S0924-2031\(02\)00065-6](https://doi.org/10.1016/S0924-2031(02)00065-6)
- Mohan, D., & Pittman, C. U. (2007). Arsenic removal from water/wastewater using adsorbents-a critical review. *Journal of Hazardous Materials*, 142(1–2), 1–53. <https://doi.org/10.1016/j.jhazmat.2007.01.006>
- Molina, C. B., Casas, J. A., Zazo, J. A., & Rodriguez, J. J. (2006). A comparison of Al-Fe and Zr-Fe pillared clays for catalytic wet peroxide oxidation. *Chemical Engineering Journal*, 118(1–2), 29–35. <https://doi.org/10.1016/j.cej.2006.01.007>
- Navalon, S., Alvaro, M., & Garcia, H. (2010). Heterogeneous Fenton catalysts based on clays, silicas and zeolites. *Applied Catalysis B Environmental*, 99(1–2), 1–26. <https://doi.org/10.1016/j.apcatb.2010.07.006>
- Official Journal of the Algerian Republic No 41 (2012). Standards for physicochemical parameters of treated wastewater for agriculture. General Secretariat of the Algerian Government, Algiers, Algeria.
- Ourari, A., Tennah, F., Ruíz-Rosas, R., Aggoun, D., & Morallón, E. (2018). Bentonite modified carbon paste electrode as a selective electrochemical sensor for the detection of cadmium and lead in aqueous solution. *International Journal of Electrochemical Science*, 13, 1683–1699. <https://doi.org/10.20964/2018.02.35>
- Ramdani, A., Taleb, S., Benghalem, A., Deratani, A., & Ghaffour, N. (2015). Enhancement of Saharan groundwater quality by reducing its fluoride concentration using different materials. *Desalination and Water Treatment*, 54(1), 3444–3453. <https://doi.org/10.1080/19443994.2014.910838>
- Ren, Y., Peng, L., Zhao, G., & Wei, C. (2014). Degradation of m-cresol via the ortho cleavage pathway by *Citrobacter farmeri* SC01. *Biochemical Engineering Journal*, 88, 108–114. <https://doi.org/10.1016/j.bej.2014.03.021>
- Saiah, O., Hachemaoui, A., & Yahiaoui, A. (2017). Synthesis of a conducting nanocomposite by intercalative copolymerisation of Furan and Aniline in Montmorillonite. *International Polymer Processing*, 32(4), 515–518. <https://doi.org/10.3139/217.3419>
- Salazar-Gil, K., Díaz-Nava, M. C., & Solache-Ríos, M. (2016). Removal of red 2 and yellow 6 by Zn- and Na modified zeolitic tuffs in the presence of H<sub>2</sub>O<sub>2</sub>. *Desalination and Water Treatment*, 57(35), 16626–16632. <https://doi.org/10.1080/19443994.2015.1079260>
- Sennour, R., Mimane, G., Benghalem, A., & Taleb, S. (2009). Removal of the persistent pollutant chlorobenzene by adsorption onto activated montmorillonite. *Applied Clay Science*, 43(3–4), 503–506. <https://doi.org/10.1016/j.clay.2008.06.019>

- Shadnia, H., & Wright, J. S. (2008). Understanding the toxicity of phenols: Using quantitative structure- activity relationship and enthalpy changes to discriminate between possible mechanisms. *Chemical Research in Toxicology*, 21(6), 1197–1204. <https://doi.org/10.1021/tx800058r>
- Shahrezaei, F., Mansouri, Y., Zinatizadeh, A. A. L., & Akhbari, A. (2012). Process modeling and kinetic evaluation of petroleum refinery wastewater treatment in a photocatalytic reactor using TiO<sub>2</sub> nanoparticles. *Powder Technology*, 221, 203–212. <https://doi.org/10.1016/j.powtec.2012.01.003>
- Shivaraman, N., & Pandey, R. (2000). Characterization and biodegradation of phenolic wastewater. *Journal of Indian Association of Environmental Management*, 27, 12–15.
- Tabué Youmbi, J. G., Feumba, R., Njitat, V. T., Marsily, G., & Ekodeck, G. E. (2013). Water pollution and health risks at Yaoundé, Cameroon. *Comptes Rendus Biologies*, 336(5–6), 310–316. <https://doi.org/10.1016/j.crvi.2013.04.013>
- Taleb, Z., Montilla, F., Quijada, C., Morallon, E., & Taleb, S. (2014). Electrochemical and in situ FTIR Study of o-Cresol on platinum electrode in acid medium. *Electrocatalysis*, 5(2), 186–192. <https://doi.org/10.1007/s12678-013-0182-x>
- Titus, E., Kalkar, A. K., & Gaikar, V. G. (2002). Adsorption of anilines and cresols on NaX and different cation exchanged zeolites (equilibrium, kinetic, and IR investigations). *Separation Science and Technology*, 37(1), 105–125. <https://doi.org/10.1081/SS-120000324>
- Toh, R. H., Lim, P. E., Seng, C. E., & Adnan, R. (2013). Immobilized acclimated biomass-powdered activated carbon for the bioregeneration of granular activated carbon loaded with phenol and o-cresol. *Bioresource Technology*, 143, 265–274. <https://doi.org/10.1016/j.biortech.2013.05.126>
- Valsania, M. C., Fasano, F., Richardson, S. D., & Vincenti, M. (2012). Investigation of the degradation of cresols in the treatments with ozone. *Water Research*, 46(8), 2795–2804. <https://doi.org/10.1016/j.watres.2012.02.040>
- Vijayakumar, J., Chikkala, S. K., Mandal, S., & Mayadevi, S. (2011). Adsorption of cresols on zinc-aluminium hydroxides—A comparison with zeolite-X. *Separation Science and Technology*, 46(3), 483–488. <https://doi.org/10.1080/01496395.2010.510494>
- Wang, Y., Wei, H., Liu, P., Yu, Y., Zhao, Y., Li, X., ... Sun, C. (2015). Effect of structural defects on activated carbon catalysts in catalytic wet peroxide oxidation of m-cresol. *Catalysis Today*, 258(1), 120–131. <https://doi.org/10.1016/j.cattod.2015.04.016>
- Wernert, V., Schaf, O., Faure, V., Brunet, P., Doub, L., Berland, Y., ... Denoye, R. (2006). Adsorption of the uremic toxin p-cresol onto hemodialysis membranes and microporous adsorbent zeolite silicalite. *Journal of Biotechnology*, 123(2), 164–173. <https://doi.org/10.1016/j.jbiotec.2005.11.009>
- William, L., & Roper, M. D. (1992). Agency for toxic substances and disease registry, Toxicological profile for cresols. U.S Public Health Service.
- Yan, Y., Wu, X., & Zhang, H. (2016). Catalytic wet peroxide oxidation of phenol over Fe<sub>2</sub>O<sub>3</sub>/MCM-41 in a fixed bed reactor. *Separation Science and Technology*, 171, 52–61.
- Yi, S., Zhuang, W. Q., Wu, B., Tay, S. T. L., & Tay, J. H. (2006). Biodegradation of p- nitrophenol by

aerobic granules in a sequencing batch reactor. *Environmental Science and Technology*, 40(7), 2396–2401. <https://doi.org/10.1021/es0517771>

Zaviska, F., Drogui, P., Mercier, G., & Blais, J. F. (2009). Advanced oxidation processes in water treatment and industrial effluent: Application to the degradation of refractory pollutants. *Reviews Water Science*, 22(1), 535–564.